Bulletin of the Seismological Society of America, Vol. 94, No. 5, pp. 1954–1959, October 2004

Short Notes

Variability of Near-Term Probability for the Next Great Earthquake on the Cascadia Subduction Zone

by Stéphane Mazzotti and John Adams

Abstract The threat of a great ($M \sim 9$) earthquake along the Cascadia subduction zone is evidenced by both paleoseismology data and current strain accumulation along the fault. On the basis of recent information on the characteristics of this subduction system, we estimate the conditional probabilities of a great earthquake occurring within the next 50 years and their variabilities. The most important variation is associated with the existence of episodic slow slip on the deep portion of the subduction interface. We show that these events modulate the conditional probability dramatically over their ~14-month cycle. During the 2-week slow-slip events, the weekly probability of a great earthquake is about 30 to 100 times as high as it is during any week of the rest of the year. Near-term probabilities also vary significantly with the assumed distribution of earthquake recurrence intervals. Under a reference scenario of unimodal distribution of recurrence intervals (about 500–600 years), the 50-year conditional probability is low (0–12% at a 95% confidence interval). However, under a tantalizing bimodal distribution hypothesis, this probability could be either four times as high (6–45%) or four times as low (less than 1%), depending on whether the current interval is short (~350 years) or long (~850 years).

Introduction

The Cascadia subduction zone is a convergent plate boundary extending over ~1000 km from northern California to southwestern British Columbia (Fig. 1). The subduction zone interface lacks current seismicity and had initially been considered unlikely to generate large earthquakes. In the 1980s and early 1990s, the threat of great (magnitude ~9) subduction earthquakes was recognized based on evidence from active geological deformation, paleoseismology, and geodetic measurements of strain accumulation (e.g., Savage *et al.*, 1981; Adams, 1984, 1985, 1990; Atwater, 1987; Rogers, 1988; Savage and Lisowski, 1991). The timing of the last great earthquake on the Cascadia subduction fault (1700 A.D.) is now well constrained by radiocarbon and tree-ring dating of coastal subsidence records (e.g., Yamaguchi *et al.*, 1997) and by Japanese records of the associated tsunami wave generated on 26 January 1700 (Satake *et al.*, 1996). Modeling of the tsunami waveform (Satake *et al.*, 1996, 2003) and of the coastal subsidence data (Leonard *et al.*, 2004) shows that the magnitude was most likely M_W ~9.

Seismic hazard assessment for the next great earthquake depends on the conditional probability of it occurring within the time period of interest (commonly, 10–100 years), which in turn is constrained by the time since the last event, the mean recurrence interval of characteristic earthquakes, and the distribution of these intervals. Previous estimates of the near-term probability yielded ~5% for the next 50 years (Adams, 1990; Adams and Weichert, 1994).

Considerable information has been gained since these estimates were made, helping constrain the age and recurrence interval of the last 13 earthquakes (compare the review in Goldfinger *et al.*, 2003). The recent discovery of episodic slow-slip events along the deep portion of the fault also provides some new insight into the temporal dynamics of this system (Dragert *et al.*, 2001; Miller *et al.*, 2002; Rogers and Dragert, 2003). In this study, we evaluate the near-term probability for the next great subduction earthquake and its variability in the light of this new information. We focus our analysis on the northern part of the Cascadia margin, where slow-slip events (and coastal earthquake records) are best documented. We investigate the variability of probability on two scales. First, we show that the conditional probability can vary significantly depending on the assumed scenario of earthquake recurrence intervals. This variation is highlighted by comparing the 50-year probability and its uncertainties for a reference scenario of unimodal interval distribution and for a tantalizing but unproven scenario of bimodal distribution (and potential clustering) of recurrence intervals. Fi-

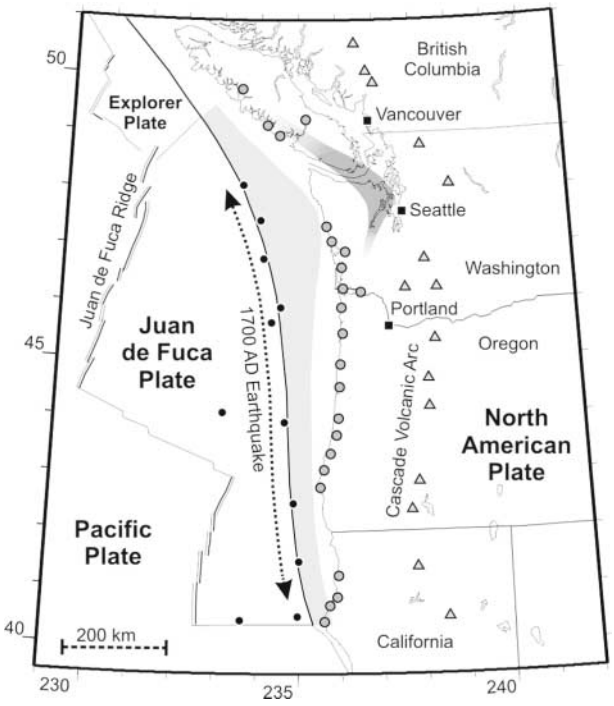

Figure 1. Cascadia subduction zone. Light shading represents the locked portion of the Cascadia subduction fault. Dark shading in northern Washington and southern British Columbia represents the detected extent of episodic slow-slip events on the deep portion of the subduction interface (Dragert *et al.*, 2001). Solid circles show the locations of offshore turbidite records (Goldfinger *et al.*, 2003). Shaded circles show the locations of coastal subsidence records of the A.D. 1700 earthquake (Leonard *et al.*, 2004).

nally, we show that, on a shorter timescale, these probabilities are strongly modulated by the occurrence of episodic slow-slip events.

Reference Case

The mean recurrence interval between great subduction earthquakes is best constrained by turbidites cored from large submarine canyons (Fig. 1). These earthquake-induced layers correlate from northern California to northern Washington and identify 13 great earthquakes during the past 7700 years (Adams, 1990). The mean recurrence interval for those earthquakes is about 600 ± 30 years, with intervals perhaps as short as 215 years and as long as 1500 years (Adams, 1990; Goldfinger *et al.*, 2003). The standard deviation of the interval distribution is ~180 years based on the thickness of sediments between the turbidites (Adams, 1990); the thickness of the turbidites themselves suggests ~105 years (Adams and Weichert, 1994). Estimates of the mean recurrence interval based on records of coastal subsidence during the subduction earthquakes vary between 440 and 590 years (e.g., Atwater and Hemphill-Haley, 1997; Nelson *et al.*, 2000; Witter *et al.*, 2003; see Fig. 2). The apparent discrepancy between the onshore and offshore estimates might be attributed to a large variation in individual interval duration being reflected in the time sampled and the number of events considered.

Assuming that the earthquake recurrence intervals, T, follow a given probability density distribution, $P(T, \langle T\rangle, \sigma)$, where $\langle T\rangle$ and σ are the mean and breadth (standard deviation, shape factor, etc.) of the distribution, and given that the earthquake has not yet occurred at time T_0, the conditional probability P_C that an earthquake will occur before time T_1 is:

$$P_C(T_1, T_0, \langle T\rangle, \sigma) = [P(T_1, \langle T\rangle, \sigma) - P(T_0, \langle T\rangle, \sigma)]/[1 - P(T_0, \langle T\rangle, \sigma)]$$

To account for the fact that the earthquake has not occurred at time T_0, the probability functions $P(T, \langle T\rangle, \sigma)$ are weighted by a factor w (Savage, 1991):

$$w = 1 - P(T_0, \langle T\rangle, \sigma)$$

Thus, the conditional probability P_C is a function of five parameters (T_1, T_0, $\langle T\rangle$, σ, and P) and the uncertainty on P_C is controlled by the uncertainties on these five parameters. For Cascadia great subduction earthquakes, T_0 is well constrained (1700 A.D.). T_1 is chosen to represent the time range of interest (in our case, 50 years). P, $\langle T\rangle$, and σ are constrained by records of coastal subsidence or offshore turbidites. We use a Monte Carlo simulation (Savage, 1991, 1992) to account for the uncertainties on these last three parameters. We estimate the means and standard deviations of $\langle T\rangle$ and σ for three possible distributions (normal, log-normal, and Weibull) and for both turbidite and coastal data sets. Assuming that $\langle T\rangle$ and σ are normally distributed, we assemble 10,000 samples of $\langle T\rangle$ and σ values for each six cases. These $\langle T\rangle$ and σ samples are used to estimate six distributions of conditional probability P_C. Combining these six distributions into one, we estimate the median and 95% confidence interval (95CI) of the "average" conditional probability.

The mean and standard deviations for $\langle T\rangle$ and σ are estimated for the three distribution functions by fitting the turbidite and coastal subsidence records using a Maximum Likelihood Estimate (MLE). Because we do not consider uncertainties on the interval durations, standard deviation estimates on $\langle T\rangle$ and σ are probably slightly underestimated. As an example, the MLE results for a normal distribution are $N(588 \pm 43, 148 \pm 30)$ and $N(517 \pm 99, 242 \pm 70)$ for the turbidite and coastal data sets, respectively (Fig. 3a,b).

For our reference scenario, the average 50-year conditional probability is low and narrowly defined: 0–12% at 95CI (median, 5%). Savage (1994) proposed a purely empirical method to derive conditional probabilities based on recurrence interval data. Applied to the turbidite data set (Adams and Weichert, 1994), the empirical 50-year condi-

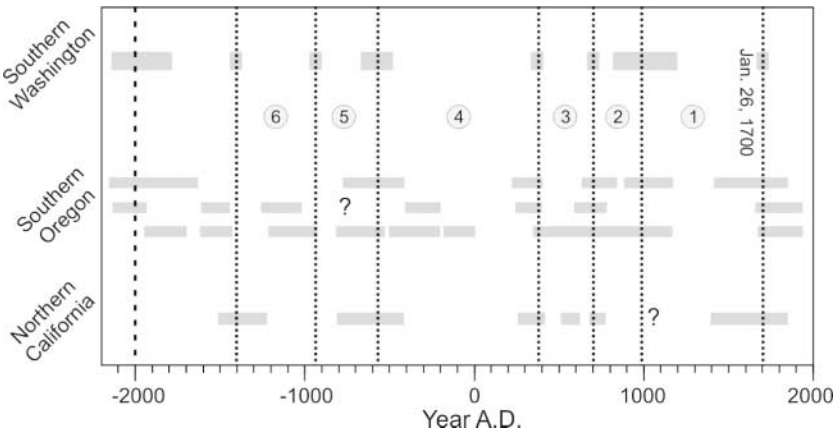

Figure 2. Timing of Cascadia subduction earthquakes for the past 4000 years. Shaded boxes represent the dates of earthquakes estimated from coastal subsidence data (compilation from Witter *et al.*, 2003). Dotted vertical lines show the average date of subduction earthquakes based on the Washington data. Note the apparent clustered distribution (short and long) of the past six recurrence intervals (number in circles).

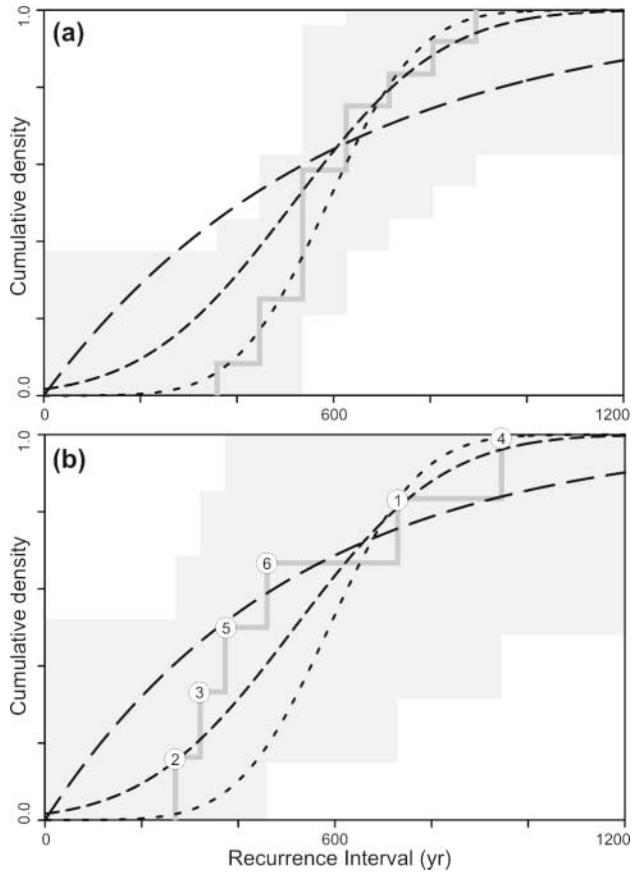

Figure 3. Recurrence interval distributions. Thick gray lines and gray shading show the distribution of earthquake recurrence intervals and 95% confidence level (Kolmogorov-Smirnov two-sided statistics). (a) Interturbidite thickness (Adams and Weichert, 1994). (b) Coastal subsidence records (numbers in Fig. 2). Short, medium, and long dashed lines show the cumulative density functions of a normal distribution $N(588, 148)$, a normal distribution $N(517, 242)$, and an exponential distribution $E(1/600)$.

tional probability is 0–19% at 95CI (median, 7%), in good agreement with our parametric estimate. The coastal subsidence data are associated with a less well constrained 50-year empirical probability (0–58% at 95CI; median, 28%). This wider probability range likely reflects uncertainties due to the small data set (six values; Fig. 2).

Impact of a Bimodal Distribution

The coastal subsidence chronology shows an interesting bimodal pattern of recurrence intervals (Fig. 2) with long (more than 700 years) and short (less than 450 years) intervals. Similarly, Jurney (2002) interpreted a slightly different data set as requiring a bimodal distribution of short (310 $\pm$ 120 years) and long (820 $\pm$ 140 years) intervals. One effect of this bimodal distribution is an apparent pattern of earthquake clustering in the coastal data, with two series of two short/one long intervals leading to the A.D. 1700 earthquake (Fig. 2). A rather similar clustering pattern has been recognized in the offshore turbidite records (Goldfinger *et al.*, 2003). The important difference is that the coastal data might suggest that the A.D. 1700 earthquake marks the beginning of a new cluster of short intervals, whereas turbidite data might suggest that the pre-1700 A.D. interval was short, perhaps indicating a long interval until the next earthquake (compare figure 4 in Goldfinger *et al.*, 2003).

Statistical tests indicate that this bimodal pattern cannot be distinguished from a unimodal distribution at the 95CI level (Fig. 3b). On statistical grounds alone it would require a long time series of reliable ages to prove that the bimodal distribution and apparent temporal clustering of great earthquake intervals are more than an unusual random sample from a unimodal distribution. However, the occurrence of clusters of large earthquakes has been suggested by paleoseismology studies in numerous plate-boundary regions (e.g., Grant and Sieh, 1994; Marco *et al.*, 1996). Fault interaction through viscoelastic stress transfer is the most common hypothesis presented to explain such clustering (e.g., Chéry *et al.*, 2001). This process could apply to the Cascadia subduction zone, where the viscoelastic mantle wedge be-

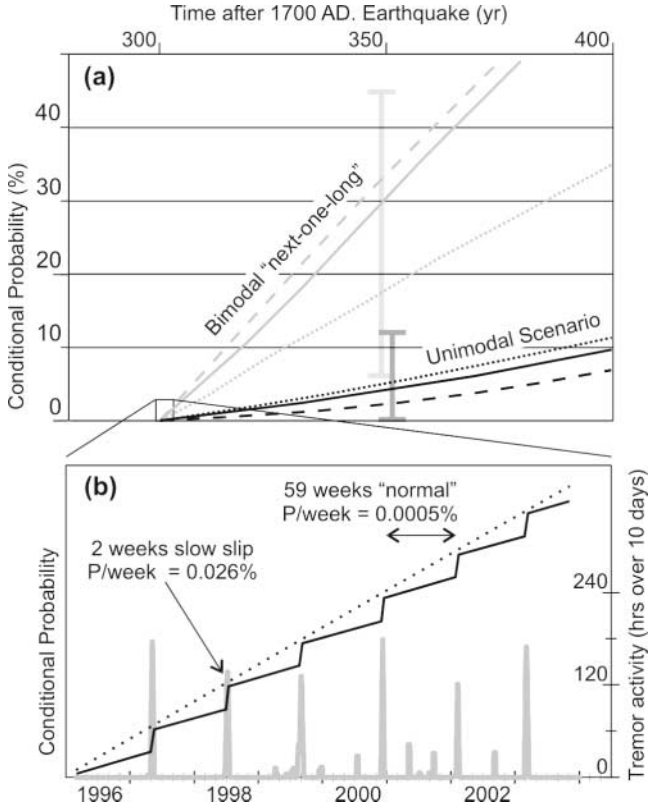

Figure 4. Conditional probabilities. (a) Conditional probability in the next $(300 - X)$ year period. Black and gray lines show probabilities for various distributions for the unimodal and bimodal "next-one-short" scenarios, respectively (solid, dotted, and dashed lines: normal, Weibull, and lognormal distributions). (b) Modulation of the probability by periodic slow-slip events. Thick gray line shows periods of tremor activity (hours over 10 days; Rogers and Dragert, 2003) as a proxy for slow-slip events. The dotted line shows the average conditional probability and the solid line shows the conditional probability modulated by slow-slip events over the past six cycles. As discussed in the text, the inter-slow-slip slope may be even flatter.

tween the subducting slab and the upper plate allows stress transfer among different faults of the subduction system, that is, segments of the subduction fault that might occasionally rupture separately (Witter *et al.*, 2003), large crustal faults in the forearc (e.g., Seattle fault), and neighboring plate boundaries (e.g., San Andreas fault). Therefore, we believe that the consequences of this unproven bimodal/cluster hypothesis are worth exploring.

As for the reference case analysis, we account for uncertainties in the bimodal "next-one-short" and the bimodal "next-one-long" scenarios with a Monte Carlo simulation of three distributions (normal, lognormal, and Weibull) with a mean $\langle T \rangle$ and breadth σ derived from a MLE analysis of the coastal subsidence data. For example, the four short and two long intervals are described by normal distributions $N(356 \pm 35, 70 \pm 25)$ and $N(850 \pm 25, 160 \pm 20)$, respectively.

Under the clustering hypothesis, we can follow the coastal data set and assume that the A.D. 1700 earthquake marks the beginning of a short interval. In this case, the 50-year conditional probability is 6–45% at 95CI (median 20%, Fig. 4a), significantly larger than for the reference scenario. On the other hand, if we assume that the current interval is long, as the turbidite data might suggest, the 50-year conditional probability becomes smaller than 1% at 95CI, reflecting the fact that we are only one-third of the way through the typical earthquake long cycle.

Alternatively, if we assume that intervals follow a bimodal distribution but are not temporally clustered (and, thus, that we don't know what the next one will be), we can combine the short- and long-interval distributions. This bimodal distribution is associated with a 50-year conditional probability of 0–40% at 95CI, with a median (1–15%) depending on the proportions of short and long intervals.

Impact of Slow-Slip Events

The recognition of slow-slip events on the deep portion of the plate interface indicates that, although strain accumulates continuously on the seismogenic part of the fault, a significant fraction of the accumulation on the deeper portion of the fault is released episodically (Dragert *et al.*, 2001). For the southern Vancouver Island-northern Washington region, these events occur about every 13–15 months (Miller *et al.*, 2002) and have a total duration of 1–3 weeks, although the duration on each part of the fault can be as short as a few days. For the last four events, modeling of the Global Positioning System (GPS) data indicates a slip amplitude of 20–40 mm and a moment release equivalent to magnitude M_W 6.6–6.9 earthquakes (Dragert *et al.*, 2001). This slip amplitude corresponds to about two-thirds of the total convergence between the Juan de Fuca and North America plates over 14 months (~45 mm).

The release of strain through slow-slip events rapidly transfers stress to the base of the seismogenic zone. Our modeling of the static stress loading suggests that a 30-mm slow-slip event increases shear stress there by about 0.001–0.005 MPa. Comparatively, the average stress drop during a subduction earthquake is 0.5–5 MPa, with the higher value occurring at the base of the seismogenic zone (Ruff, 1999), where the slow-slip events cause the largest loading. Assuming a 600-year earthquake cycle, this suggests an average loading rate on the deep part of the seismogenic zone of about 0.001–0.01 MPa per 14 months. Thus, the incremental loading during a 2-week slow-slip event represents a significant part (half or more) of the total accumulation during the 14-month cycle.

The probability per week of a great subduction earthquake occurring during or outside of a slow-slip event (SSE) period is given by:

$$P_W = \alpha P_C(T_{SSE})/t_{SSE}, \quad \text{during slow-slip event}$$

$$P_W = (1 - \alpha)\, P_C(T_{SSE})/(T_{SSE} - t_{SSE}), \quad \text{outside slow-slip event}$$

where T_{SSE} and t_{SSE} are the interevent period and the duration of slow-slip, and α is the ratio of shear stress loading on the seismogenic zone during an event to the total loading during an interevent period. For northern Cascadia, we use $t_{SSE} = 2 \pm 1$ weeks, $T_{SSE} = 58 \pm 4$ weeks, and $\alpha = 0.65 \pm 0.2$.

Based on these expressions, the probability per week of a great subduction earthquake occurring during a slow-slip event is about 30–100 times as high as outside of the slow-slip period. For our reference case, the average conditional probability is ~0.026% (~1/4000) during one of the next slow-slip weeks compared with ~0.0005% (~1/200,000) for any other week (Fig. 4b). Similarly, slow-slip modulation applied to the clustering scenario leads to a weekly probability of ~0.21% (~1/500) during slow slip versus ~0.004% (~1/25,000) outside slow slip.

This analysis is subject to large uncertainties and is probably conservative because (1) seismic failure may be partly related to the rate of stress change, in which case the chance of rupture during the slow-loading 58-week period may be closer to 0% than to 33%, and the fast-loading slow-slip period probabilities increase by 50%; (2) the loading rates cited previously may be low by a factor of 2 or more because the slow-slip events typically last for less than 1 week in any one place (Dragert *et al.*, 2001; Rogers and Dragert, 2003). However, because we do not know *ab initio* where the earthquake will start, we must consider the entire 2-week window as being hazardous; and (3) although not clearly identified yet, potential slow-slip events in central and southern Cascadia (Szeliga *et al.*, 2003) or in northernmost Cascadia (Rogers *et al.*, 2004) might interfere with stress loading along the northern section of the subduction fault (thus changing the short-term modulation of probabilities).

Conclusions

The most important conclusion of this study is that the recently discovered deep slow-slip events on the Cascadia subduction zone dramatically modulate the probability of a great subduction earthquake. During the 2-week slow-slip events, the weekly probability of a great earthquake is about 30–100 times as high as at other times. This slow-slip modulation could be significantly larger if there is stress-rate dependence of earthquake initiation. A slow-slip episode might be predicted months ahead based on past periodicity and its commencement can be confirmed from a combination of GPS and episodic tremor evidence (Rogers and Dragert, 2003) about 48 hr after it has begun. If our conclusions about slow-slip impact on hazard are confirmed, the prediction could be used for pre-event campaigns of public earthquake awareness. Rapid confirmation of a slow-slip event could allow emergency-measures organizations to implement selected disaster mitigation activities during the remainder of the event duration.

The near-term conditional probabilities for a great Cascadia earthquake are also extremely sensitive to the assumed distribution of recurrence intervals. Assuming a unimodal distribution (mean, 500–600 years), the 50-year conditional probability is 0–12% at 95CI. Under a temporal-clustering hypothesis, this probability could raise to 6–45% or drop to less than 1% if the current interval is short (~350 years) or long (~850 years). The difference between these three estimates is not only highly significant for probabilistic hazard assessment, it may also have important behavioral impact, because some people might consider a 1/5 chance more seriously than a 1/20 chance. From our analysis, the bimodal distribution and apparent temporal clustering of great earthquakes in the coastal data is not statistically significant. This illustrates the importance paleoseismic studies to assess whether earthquakes cluster in time, the temporal properties of the clusters, and the expected duration of the post-1700 A.D. interval in which we live.

Acknowledgments

We thank our Geological Survey of Canada colleagues G. Rogers, H. Dragert, and R. Hyndman for discussions and comments. Reviews by J. Savage and K. Wang helped improve and clarify the manuscript. This is Geological Survey of Canada Contribution no. 2003302.

References

Adams, J. (1984). Active deformation of the Pacific Northwest continental margin, *Tectonics* **3,** 449–472.

Adams, J. (1985). Deformation above the Juan de Fuca subduction zone: some enigma with bearing on great-earthquake risk, *EOS Trans.* **66,** 1071.

Adams, J. (1990). Paleoseismicity of the Cascadia subduction zone: evidence from turbidites off the Oregon-Washington margin, *Tectonics* **9,** 569–583.

Adams, J., and D. Weichert (1994). Near-term probability of the future Cascadia megaquake. *U.S. Geol. Surv. Open-File Rept. 94-568*, 3 pp.

Atwater, B. F. (1987). Evidence for great Holocene earthquakes along the outer coast of Washington State, *Science* **236,** 942–944.

Atwater, B. F., and E. Hemphill-Haley (1997). Recurrence intervals for great earthquakes of the past 3500 years at northeastern Willapa Bay, Washington, *U.S. Geol. Surv. Profess. Pap. 1576*, 108 pp.

Chéry, J., S. Carretier, and J. F. Ritz (2001). Postseismic stress transfer explains time clustering of large earthquakes in Mongolia, *Earth Planet. Sci. Lett.* **194,** 277–286.

Dragert, H., K. Wang, and T. S. James (2001). A silent slip event on the deeper Cascadia subduction interface, *Science* **292,** 1525–1528.

Goldfinger, C., C. H. Nelson, and J. E. Johnson (2003). Holocene earthquake records from the Cascadia subduction zone and northern San Andreas Fault based on precise dating of offshore turbidites, *Annu. Rev. Earth Planet. Sci.* **31,** 555–577.

Grant, L., and K. Sieh (1994). Paleoseismic evidence of clustered earthquakes on the San Andreas fault in the Carrizo plain, California, *J. Geophys. Res.* **99,** 6819–6841.

Jurney, C. (2002). Recurrence of great earthquakes: evidence of double periodicity along the Cascadia subduction zone (abstract S22B-1039). *EOS Trans.* **83,** Fall Meeting Suppl.

Leonard, L., R. D. Hyndman, and S. Mazzotti (2004). Coseismic subsidence in the 1700 great Cascadia earthquake: Geological estimates versus geodetically controlled elastic dislocation models, *GSA Bull.*, **116,** doi 10.1130/B25369.1.

Marco, S., M. Stein, and A. Agnon (1996). Long term earthquake clustering: a 50,000-year paleoseismic record in the Dead Sea graben, *J. Geophys. Res.* **101,** 6179–6191.

Miller, M. M., T. Melbourne, D. J. Johnson, and W. Q. Sumner (2002). Periodic slow earthquakes from the Cascadia subduction zone, *Science* **295,** 2423.

Nelson, A. R., H. M. Kelsey, E. Hemphill-Haley, and R. C. Witter (2000). Oxcal analyses and varve-based sedimentation rates constrain the times of c14 dated tsunamis in southern Oregon, in *Proc. GSA Penrose Conf. Great Cascadia Earthquake Tricentennial*, Portland, Oregon, Oregon Dpt. Geol. Miner. Ind., 71–72.

Rogers, G. C. (1988). Seismic potential of the Cascadia subduction zone, *Nature* **332,** 17.

Rogers, G. C., and H. Dragert (2003). Episodic tremor and slip on the Cascadia subduction zone: the chatter of silent slip, *Science* **300,** 1942–1943.

Rogers, G. C., J. F. Cassidy, and H. Dragert (2004). Episodic tremor and slip (ETS) beneath Vancouver Island, Canada. *Seism. Res. Lett.* **74,** 241.

Ruff, L. J. (1999). Dynamic stress drop of recent earthquakes: variations within the subduction zones, *Pure Appl. Geophys.* **154,** 409–431.

Satake, K., K. Shimazaki, Y. Tsuji, and K. Ueda (1996). Time and size of a giant earthquake in Cascadia inferred from Japanese tsunami record of January, 1700, *Nature* **379,** 246–249.

Satake, K., K. Wang, and B. F. Atwater (2003). Fault slip and seismic moment of the 1700 Cascadia earthquake inferred from Japanese tsunami description, *J. Geophys. Res.* **108,** doi 10.1029/2003JB002521.

Savage, J. C. (1991). Criticism of some forecasts of the National Earthquake Prediction Evaluation Council, *Bull. Seism. Soc. Am.* **81,** 862–881.

Savage, J. C. (1992). The uncertainty in earthquake conditional probabilities, *Geophys. Res. Lett.* **19,** 709–712.

Savage, J. C. (1994). Empirical earthquake probabilities from observed recurrence intervals, *Bull. Seism. Soc. Am.* **84,** 219–221.

Savage, J. C., and M. Lisowski (1991). Strain measurements and potential for a great subduction earthquake off the coast of Washington, *Science* **252,** 101–103.

Savage, J. C., M. Lisowski, and W. H. Prescott (1981). Geodetic strain in Washington, *J. Geophys. Res.* **86,** 4929–4940.

Szeliga, W. M., T. I. Melbourne, M. M. Miller, V. M. Santillan, and W. Sumner (2003). Evidence for Cascadia-Wide Rupture of Episodic Slow Earthquakes, *Eos Trans. AGU* **84,** S42G-04.

Witter, R. C., H. M. Kelsey, and E. Hemphill-Haley (2003). Great Cascadia earthquakes and tsunamis of the past 6700 years, Coquille River estuary, southern coastal Oregon, *Geol. Soc. Am. Bull.* **115,** 1289–1306.

Yamaguchi, D. K., B. F. Atwater, D. E. Bunker, B. E. Benson, and M. S. Reid (1997). Tree-ring dating the 1700 Cascadia earthquake, *Nature* **389,** 922–923.

Geological Survey of Canada
9860 West Saanich Road
Sidney BC, V8L4B2, Canada
smazzotti@NRCan.gc.ca
(S.M.)

Geological Survey of Canada
7 Observatory Crescent
Ottawa, ON, K1A0Y3, Canada
adams@seismo.nrcan.gc.ca
(J.A.)

Manuscript received 26 February 2004.